

Design & Analysis of Miniaturized Asymmetric Coplanar Strip Fed Antenna for Multi-Band WLAN/WiMAX Applications

Praveen V. Naidu* and Akshay Malhotra

Abstract—A novel, compact asymmetric coplanar strip (ACS)-fed multi-band antenna for Bluetooth/WLAN/WiMAX applications is proposed and discussed in this paper. The proposed antenna is composed of a simple monopole structure with a mirror-L shaped branch and two rectangular radiating strips. It has a very small size of $13.75 \times 26 \text{ mm}^2$ including the ground plane. The mirror-L shaped branch excites a resonant mode at 2.5 GHz, and on the other side, ACS-fed monopole structure with two rectangular strips (one horizontal and one vertical) excite the resonant modes at 3.3 GHz and 5.75 GHz respectively. By properly selecting the lengths and positions of these radiating branches, multiband operation with wider impedance bandwidth can be achieved. The measured and simulated results show that the antenna has impedance bandwidth of 200 MHz (2.40–2.60 GHz), and 2800 MHz (3.2–6.0 GHz), and it can cover the 2.4 GHz Bluetooth, 2.4/5.2/5.8 GHz WLAN and 3.5/5.5 GHz WiMAX bands. The resonances achieved with this technique can be tuned independently, and the equations governing the resonances are given and confirmed by parametric studies. The proposed technique is further validated by designing another antenna working at 1.8/1.9 GHz PCS, 3.5/5.5 GHz WiMAX, 5.2/5.8 GHz WLAN bands.

1. INTRODUCTION

Nowadays, the demand for using Wireless Local Area Network (WLAN: 2.4–2.48, 5.15–5.35, and 5.72–5.85 GHz) and Worldwide Interoperability for Microwave Access (WiMAX: 3.40–3.69, and 5.25–5.85 GHz) protocols has increased drastically because of its highend features such as cost effectiveness, wire free connectivity and short distance high speed data transfer technology. This has intensified the need for multi-band antennas that work at these frequencies. Along with the multi-band feature, compactness is also required because of the limited space availability for an antenna element in all modern communication devices (like mobile phones, portable laptops and handheld electronic gadgets). So designing an antenna that supports 2.4/3.5/5.2/5.5/5.8 GHz communication standards with compact size has attracted significant attention. Various types of printed multi-band antennas have been reported, such as monopole antenna with L- and E-shaped radiators [1], triangle-shaped antenna with Π -shaped slot and T-shaped strip [2], rhombus slot antenna [3], L-shaped radiator with M-shaped stub in the ground plane [4], Bow-Tie shaped slot antenna [5], slotted rectangular patch antenna [6], rectangular patch with meandered slit [7], asymmetric coplanar strip (ACS)-fed F-shaped antenna [8], CPW-fed slot antenna [9], ring monopole antenna with double meandered lines [10], ACS-fed slot antenna [11]. Some of the reported antennas [1–11] perform well in the radiation characteristics, but they operate in only WLAN band. Also, most of them have large size making it difficult to integrate in the miniaturized communication devices. So there is a demand for designing compact multi-band antennas having wideband characteristics.

To cover the WLAN and WiMAX application standards simultaneously, several other antennas have been reported [12–26]. For example, a tri-band antenna with rectangular ring, S- and U-shaped strips for

Received 23 April 2015, Accepted 29 May 2015, Scheduled 4 June 2015

* Corresponding author: Praveen Vummadisetty Naidu (praveennaidu468@gmail.com).

The authors are with the Centre for Radio Science Studies, Symbiosis International University, Lavale, Pune 412115, India.

WLAN and WiMAX applications is presented [12], and a novel rupee-shaped CPW-fed antenna in [13], and an octagonal shaped slot antenna in [14] are reported for dual/tri-band applications. A rectangular ring patch monopole antenna with two inverted L-shaped strips [15], rectangular patch antenna with U-shaped slots [16], in [17], triple-band operation is achieved with L-shaped slot cut in the radiating patch and an inverted L-shaped stub in the ground plane. Rhombus slot antenna is reported in [18], circular patch with L-shaped slots in [19], hybrid strips monopole antenna in [21], a microstrip antenna with open-ended slot on the ground plane in [22], triangular shaped monopole dual-band antenna in [23], and a novel compact omega shaped ACS-fed antenna in [24]. To reduce the size, some other compact antennas designed using the concept of ACS-fed are given in [26–32]. Although some of the reported antennas [27–30] are compact in size, most of them operate at limited frequencies in WLAN/WiMAX bands. For example an antenna reported in [27] covers only 3.5/5.8 GHz application bands; antennas in [28, 29] covers only 2.4/5.8 GHz WLAN band; an antenna reported in [30] covers only 2.4/5.8 GHz WLAN and 3.5 GHz. WiMAX bands. In Table 1, a comparison of tri-band antennas in terms of antenna size, application, total area occupied by the antenna, its frequency of operation and average peak gains has been given. From the table it can be seen that the proposed antenna is the smallest covering maximum number of bands and applications and has a comparable if not higher gain. Majority of the reported antennas have drawbacks of large size and/or limited frequency of operation compared with our proposed design. The proposed antenna also has a simple structure with independent tunability of resonant frequency which other designs rarely offer.

Table 1. Comparison of proposed antenna performance with other multi-band antennas.

Published literature	Antenna size (mm ²)	Total area occupied (mm ²)	Antenna Purpose		Avg Peak gain (dBi)
			WLAN	WiMAX	
[12]	35 × 25	875	2.4/5.2/5.8 GHz	3.5/5.5 GHz	2.4
[16]	25 × 18	450	2.4/5.2/5.8 GHz	3.5/5.5 GHz	3.7
[17]	17 × 30	510	2.4/5.2/5.8 GHz	3.5/5.5 GHz	2.0
[19]	22 × 41	902	2.4/5.2/5.8 GHz	3.5 GHz	3.5
[20]	40 × 40	1600	2.4/5.2/5.8 GHz	3.5/5.5 GHz	3.3
[21]	38 × 20	760	2.4/5.8 GHz	3.5 GHz	3.1
[22]	14 × 34	476	2.4/5.8 GHz	3.5 GHz	1.7
[25]	18 × 28	504	2.4/5.2/5.8 GHz	3.5/5.5 GHz	2.7
[26]	35 × 19	665	2.4/5.2/5.8 GHz	3.5/5.5 GHz	3.6
[30]	26.5 × 12	318	2.4/5.8 GHz	3.5 GHz	2.0
Proposed antenna	13.75 × 26	357.5	2.4/5.2/5.8 GHz	3.5/5.5 GHz	3.25

In this paper, a compact multiband antenna fed by an asymmetrical coplanar strip (ACS) for WLAN/WiMAX applications is proposed. The antenna consists of an mirror-L shaped branch and two rectangle-shaped stubs connected with monopole structure. The measured operating bandwidths of the proposed antenna are about 200 MHz and 2800 MHz, respectively, which satisfies the 2.4/5.2/5.8 GHz wireless local area network (WLAN) and 3.5/5.5 GHz worldwide interoperability for microwave access (WiMAX), and 2.4 GHz Bluetooth/RFID/WiBree/ZigBee bands. The details of antenna evolution process, parametric studies, experimental radiation patterns and peak gains are given in the following sections.

2. ANTENNA EVOLUTION & DESIGN

Figure 1 shows the configuration and photograph of the proposed ACS-fed monopole multi-band antenna designed for 2.4/5.2/5.8 GHz WLAN and 3.5/5.5 GHz WiMAX applications. The antenna is printed on a 13.75 × 26 mm² low-cost FR4 substrate having thickness of 1.6 mm, dielectric constant of 4.4 and loss tangent $\tan \delta = 0.02$. Like CPW-feeding technique, a 50 ohm asymmetric coplanar strip transmission

line of width $L_1 = 3.3$ mm, with a gap distance of $g_2 = 0.45$ mm between the signal strip and ground plane, is considered for feeding the antenna. The electromagnetic simulation software CST microwave studio package is used for design and analysis of the proposed antenna. The optimized dimensions of the proposed antenna are given as follows: $W = 26$, $L = 13.75$, $W_1 = 4.5$, $W_2 = 3$, $L_2 = 10$, $W_3 = 3.5$, $L_3 = 2.7$, $W_4 = 13.6$, $L_4 = 8.2$, $W_5 = 2$, $L_5 = 3$, $L_6 = 3.4$, $g = 1.4$ and $g_1 = 1.7$ (all values are in mm).

The process of designing the proposed multi-band antenna is shown in Figure 2, and its corresponding frequency versus reflection coefficient curves are given in Figure 3. Antenna #1 and Antenna #2 are the original ACS-fed monopole structures, which consist of a pair of mirror-L shaped branches with width of 0.8 mm and a vertical rectangular stub with width of 1.7 mm, respectively. From Figure 3, it can be seen that there are two independent resonant modes, one at 2.5 GHz WLAN band due to mirror-L shaped branches and the other at 3.4 GHz WiMAX band due to rectangular stub. The next step is to integrate Antenna #1 and Antenna #2 structures (Antenna #3) to excite two simultaneous resonant modes. As illustrated in Figure 3, (blue color), Antenna #3 covers the operating band from 2.4–2.65 GHz and from 3.2–3.9 GHz. Meanwhile, the weak harmonics are located at 4.75 GHz and 6.0 GHz. Next step is to modify Antenna #3, so as to make it suitable for 5.2/5.8 GHz WLAN and 5.5 GHz WiMAX applications. This is achieved by adding a quarter wavelength rectangular (horizontal) radiating element to Antenna #3. The resulting antenna structure is shown as proposed antenna in Figure 2. By adding rectangular stub to the monopole (red color), the third resonant mode at 5.75 GHz can be achieved. The newly added structure hardly affects resonant frequencies that were achieved

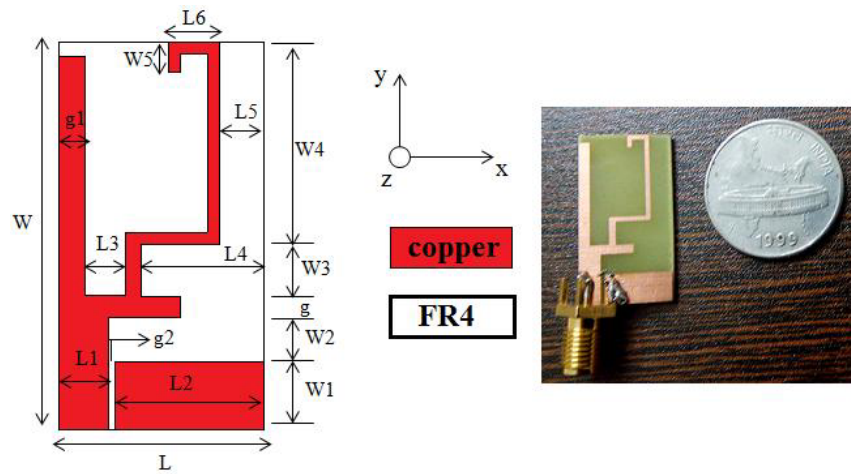


Figure 1. Geometry and fabricated photograph of the proposed ACS-fed antenna.

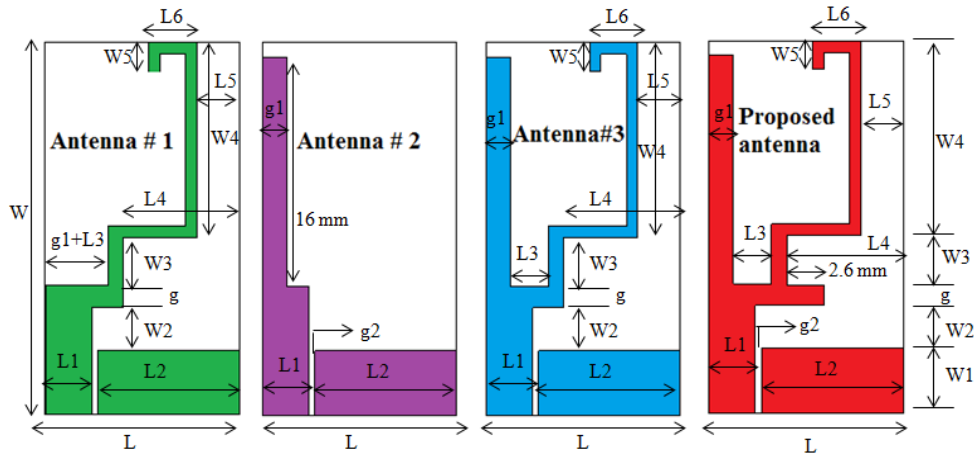


Figure 2. Geometry of various antennas involved in the design evolution process.

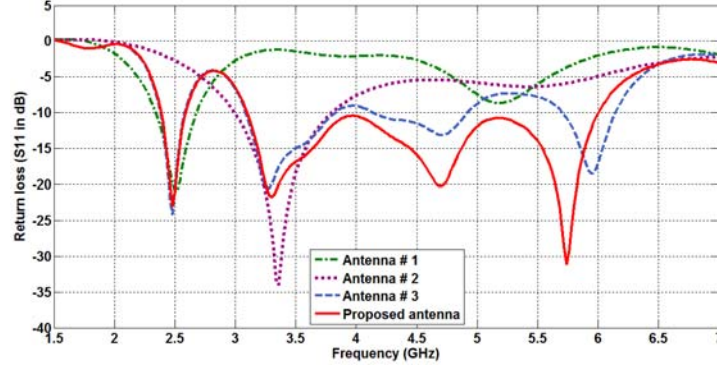


Figure 3. Simulated return loss curves of antennas involved in the design evolution process.

before. Also due to the strong harmonics, the second and third resonant bands are merged and form, a wide band with improved return loss characteristics. Therefore, the proposed antenna with operating bands from 2.4–2.6 GHz and 3.1–6.0 GHz for WLAN/WiMAX applications is obtained.

3. RESULTS AND DISCUSSION

The proposed multi-band antenna with optimized dimensions is fabricated, and its return loss characteristics are validated experimentally by using R&S ZVA 40 vector network analyzer. It can be seen from Figure 4(a) that the simulated and measured results show good agreement. The measured -10 dB impedance bandwidths are about 200 MHz (2.40–2.60 GHz) resonated at 2.5 GHz, and 2800 MHz (3.2–6.0 GHz) resonated at 3.7 GHz and 5.75 GHz, respectively, which can be used for 2.4 GHz Bluetooth, 2.4/5.2/5.8 GHz WLAN and 3.5/5.5 GHz WiMAX bands. The slight difference between simulated and measured results is probably due to manufacturing tolerances, uncertainty of the thickness and/or the dielectric constant of the FR4 substrate and quality of SMA connector used.

In case of compact antennas, the currents may flow in external co-axial ground of connector and cable, which may disturb the return loss. So the proposed antenna is also simulated by considering the effect of coaxial cable with SMA connector having dimensions that correspond to the actual connector and cable used for measurements. In the CST software, the SMA connector is modeled using three coaxial cylinders of length 10 mm (as shown in Figure 8 and Figures 4(b), (c), (d)) with an appropriate radius. The inner conductor of the cable has a radius of 0.65 mm; the outer conductor has an inner radius of 2.25 mm and an outer radius of 2.5 mm; the dielectric Teflon with a permittivity of 2.1 is used to fill the space between inner and outer conductors. The co-axial cable connecting SMA connector to VNA is also modeled to study its effect on return loss (given in Figure 4(a)) and surface current distribution (given in Figures 4(b), (c), (d)) on outer conductor of the cable. From Figure 4(a) it can be observed that almost a similar return loss result can be observed with and without considering cable that was connected to SMA connector in the simulation. Also in Figures 4(b), (c), (d), a very small amount of current flows on the outer surface of the cable, which leads to negligible unbalanced currents in coaxial cable. This explains the reason for good agreement between the simulated and measured results.

The measured far-field radiation patterns in E -plane and H -plane at 2.45 GHz, 3.7 GHz. and 5.75 GHz are shown in Figure 5. A standard double ridged horn antenna is used as a reference antenna in the antenna measurement system. Nearly bi-directional radiation patterns in E -plane and omnidirectional patterns in H -plane are observed over the operating band frequencies. The simulated and measured radiation patterns are in good agreement, with a little difference due to measurement and alignment errors. Figure 6 shows the measured peak gains across multi operating bands. The average peak gain across all the operating bands is 3.25 dBi. It can be seen from Figure 5 that the orthogonal polarization (cross polarization) at the third frequency is slightly more than those at other two frequencies. It can be because of the orientation of L shape which is responsible for third resonance; however, the polarization is largely determined by the ground plane just like in IFA antenna [33]. So co-polar component still corresponds to the same polarization as at other two frequencies. The radiation

efficiency characteristics of the proposed antenna were calculated by using CST Microwave Studio. In the first operating band, the radiation efficiency is about 71% while in the second operating band it is about 82%. At smaller frequencies, the antenna becomes smaller than the wavelength. Hence, the antenna becomes more like a transmission line than as a radiating element. So, even when the return loss is better, the part of the energy radiated becomes less. Hence, the efficiency is less at lower frequencies.

4. PARAMETRIC STUDIES

To further investigate the multi/wide band characteristics of the proposed antenna, some important parametric studies are carried out and given in Figures 7(a), (b) and (c), respectively. The effects of varying the parameter X_1 on return loss are given in Figure 7(a). It can be observed from the figure that as the length of the mirror-L shape ladder branch ' X_1 ' decreases, the first resonant frequency shifts towards higher frequencies. At the same time the upper frequency limit of second operating band slightly varies accordingly. Figure 7(b) plots the simulated return loss curves by changing the length of the vertical rectangular stub ' Y_1 '. It can be seen that as the length decreases, the second resonant frequency (3.3 GHz) shifts to higher side with minimal effect on the first frequency band. As a result, the overall impedance bandwidth of the second operating band decreases. Hence an optimized value of $Y_1 = 15$ mm is considered in the final design.

Figure 7(c) describes the simulated return losses when the length of the horizontal rectangular strip Z_1 varies from 1.6 mm to 3.6 mm. It can be seen that as the Z_1 increases, the third resonant frequency shifts towards lower frequencies, while the first and second operating bands are almost unchanged. Also it is observed that as the value of Z_1 decreases the return loss near third operating band deteriorates. Hence an optimized value of $Z_1 = 2.6$ mm is considered in the final design. From the above results it can be concluded that the three resonant frequencies and their impedance bandwidth can be tuned and controlled independently by adjusting the dimensions of the parameters X_1 , Y_1 and Z_1 .

The effect of the asymmetric ground plane dimensions (W_1 and L_2) on the proposed antenna performance is studied and given in Figures 7(d) and (e). Figure 7(d) illustrates the simulated return

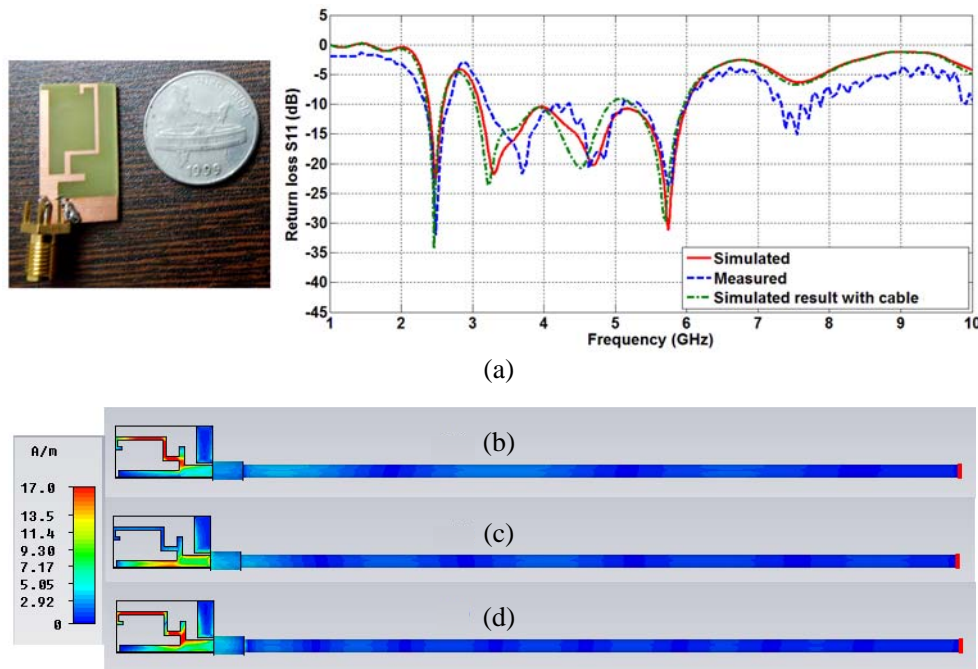


Figure 4. (a) Photograph of the fabricated prototype and comparison of simulated and measured return losses against frequency. (b), (c), (d) Simulated surface current distribution of proposed antenna with cable attached (b) 2.5 GHz, (c) 3.3 GHz, and (d) 5.7 GHz.

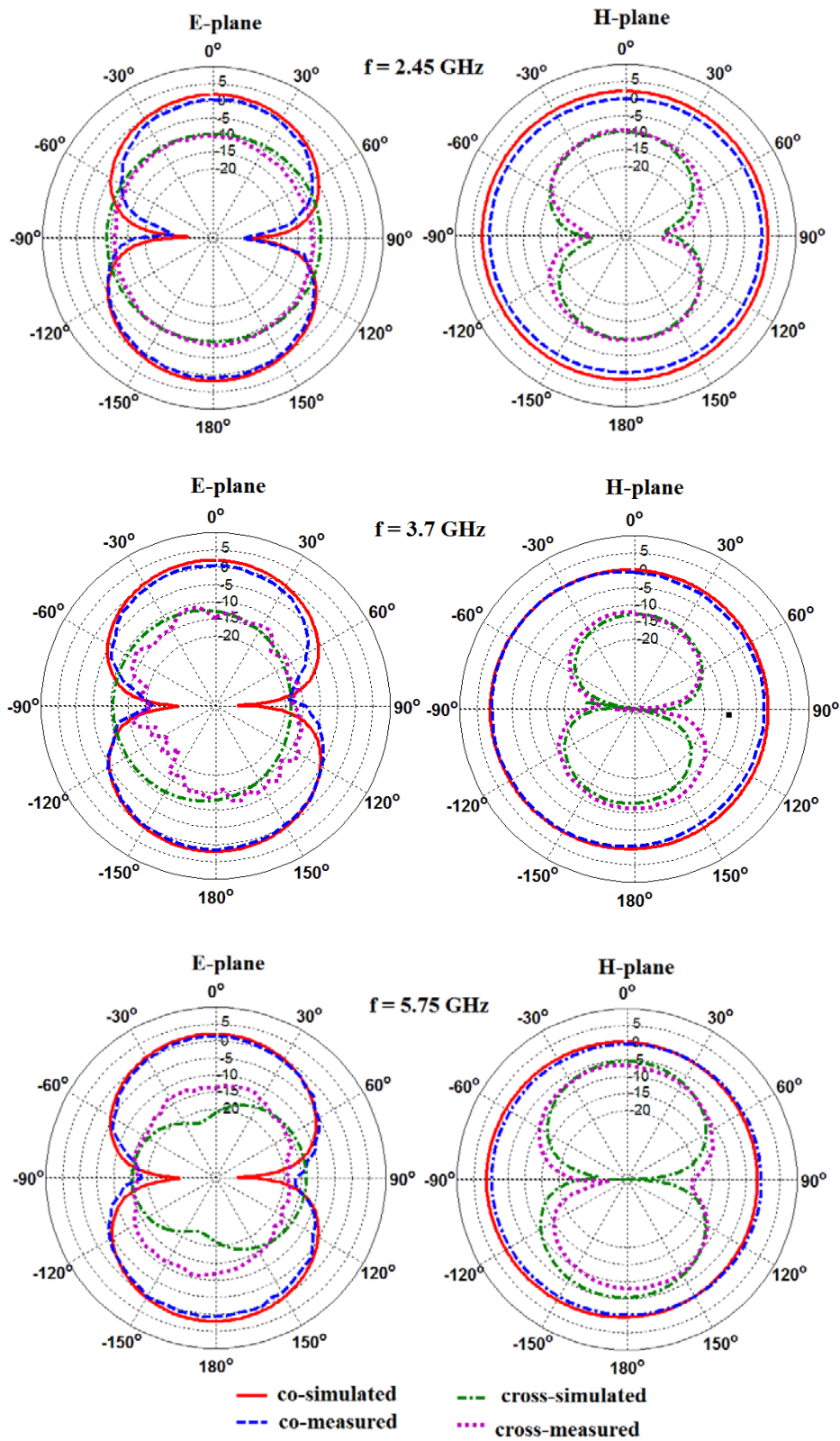


Figure 5. Measured and simulated radiation patterns of the proposed ACS-fed tri-band antenna at 2.45 GHz, 3.7 GHz and 5.75 GHz.

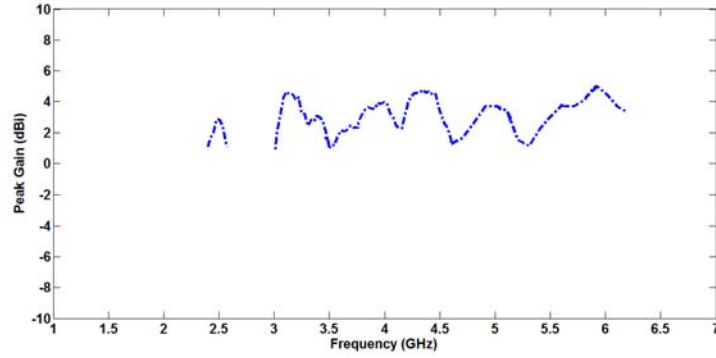


Figure 6. Measured peak gain of the proposed antenna.

loss curves for different values of W_1 . It can be observed from the figure that with the increase of W_1 , the return loss characteristics of the the second operating band are improved due to the coupling between the radiating element (horizontal strip) and ground plane. Similarly, Figure 7(e) describes the simulated return losses when the length of the ground plane L_2 varies from 10 mm to 9 mm. As the parameter L_2 decreases, the return loss characteristics of the second operating band are strongly affected, which means that the antenna impedance bandwidth also depends on the asymmetric ground plane. Hence to achieve wider impedance bandwidth and good return loss characteristics, the optimum ground plane dimensions of $W_1 = 4.5$ mm and $L_2 = 10$ mm are chosen in the final design.

The parametric studies have shown that the resonant frequencies are independently tunable by changing the geometry parameters. For investigating the study of the propped ACS-fed antenna, the simulated surface current distributions at resonant frequencies of 2.5 GHz, 3.3 GHz, and 5.75 GHz are presented in Figure 8. In the figure, red color indicates maximum current density while blue color indicates minimum current density. For 2.5 GHz excitation, a large surface current is observed on the mirror-L shaped ladder branch ($H_1 = \text{patch 'abcdef'} = 36$ mm) of the monopole. This indicates that mirror-L shaped ladder branch ($\lambda/2$) acts as a resonator to generate lower resonance. At 3.3 GHz, most of the surface currents shown in Figure 8 concentrate along the vertical rectangular stub ($Y_1 = \text{path 'gh'} = 14.5$ mm). This indicates that the second resonant mode is generated due to the quarter wavelength ($\lambda/4$) structure. For 5.75 GHz excitation, it can be seen from the figure that the maximum currents are distributed on the quarter wavelength ($\lambda/4$) horizontal rectangular strip ($H_2 = \text{path 'xyz'} = 7.8$ mm), and thus the upper resonant mode at 5.8 GHz for WLAN application is achieved. The expression for the same can be given in Equations (1)–(4). All the three resonant frequencies can be tuned independently by varying the lengths of each of the individual radiating strips.

$$f_1 = \frac{c}{2H_1\sqrt{\epsilon_{r,eff}}} \tag{1}$$

$$f_2 = \frac{c}{4Y_1\sqrt{\epsilon_{r,eff}}} \tag{2}$$

$$f_3 = \frac{c}{4H_2\sqrt{\epsilon_{r,eff}}} \tag{3}$$

$$\epsilon_{r,eff} = \frac{\epsilon_r + 1}{2} \tag{4}$$

Table 2. Comparison of calculated and simulated frequencies of the propose antenna.

	f_1 (GHz)	f_2 (GHz)	f_3 (GHz)
Calculated	2.54	3.15	5.86
Simulated	2.48	3.28	5.74
Measured	2.50	3.70	5.75

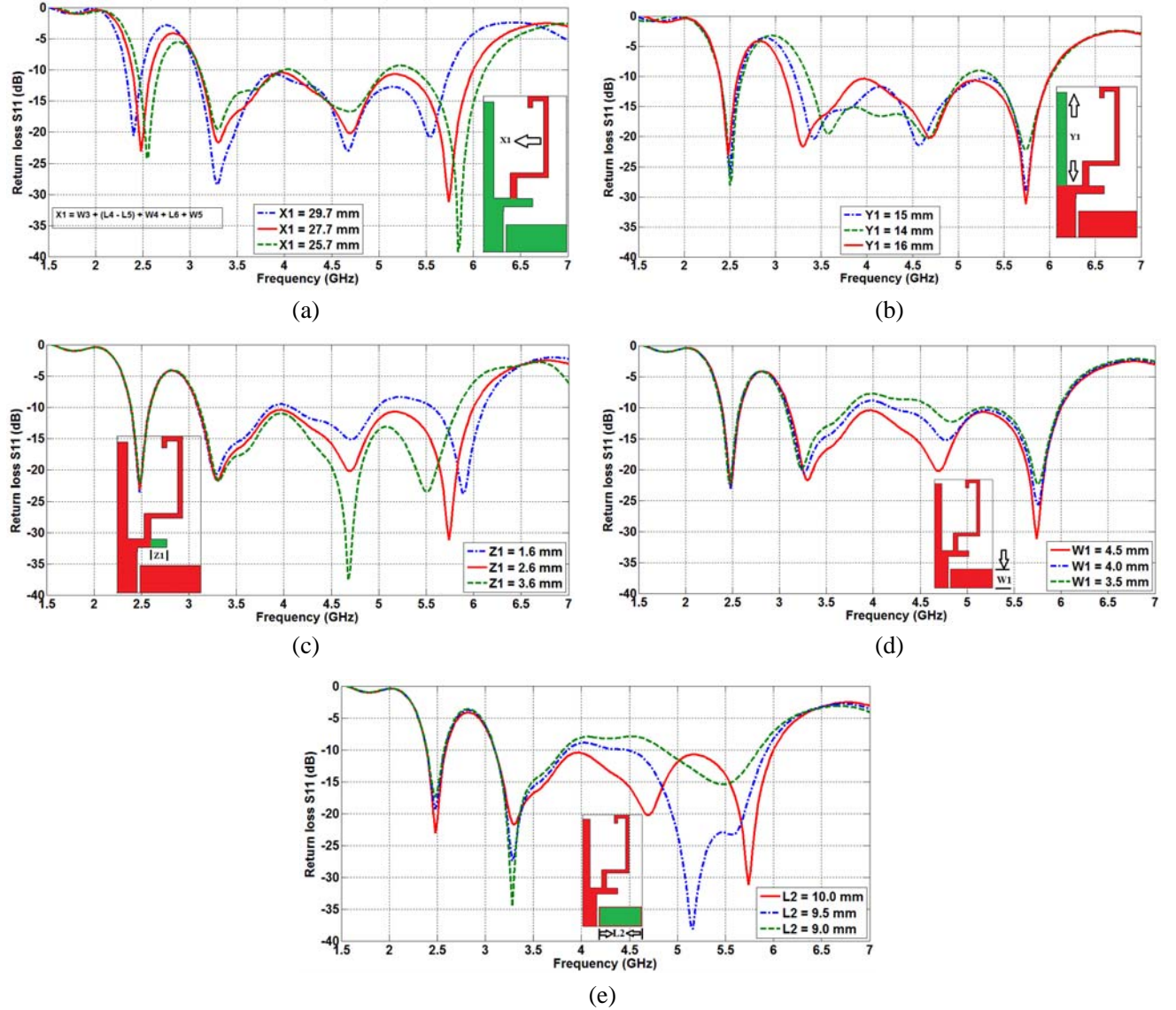


Figure 7. (a) Simulated return losses of the proposed antenna for various X_1 . (b) Simulated return losses of the proposed antenna for various Y_1 . (c) Simulated return losses of the proposed antenna for various Z_1 . (d) Simulated return losses of the proposed antenna for various W_1 . (e) Simulated return losses of the proposed antenna for various L_2 .

where c stands for the velocity of light in free space, and $\epsilon_{r,eff}$ is the effective relative permittivity of the substrate which can be calculated from Equation (4). For calculating the effective relative permittivity, it is assumed that for a ACS-fed monopole, half of the established field lies in air while the remaining half is distributed in the substrate. Table 2 shows the comparison of the resonances calculated using above equations and those obtained by simulation. The close agreement of the measured, simulated and calculated results along with current distribution confirms the correctness of the proposed equations.

5. VALIDATION OF PROPOSED TECHNIQUE — ARC STRIP ANTENNA

In order to validate the proposed design strategy, another similar tri-band antenna is designed, simulated and analyzed. The geometry of the new tri-band monopole antenna fed by an asymmetric coplanar strip is shown in Figure 9. The tri-band antenna is composed of an arc-shaped monopole strip, a rectangular-

shaped branch, and an L-shaped strip attached to the feed line. The three operating bands are obtained from the excitation of resonances due to these strips. The antenna is designed and printed on a $17.2 \times 30 \text{ mm}^2$ size FR4 substrate having dielectric constant 4.4, thickness 1.6 mm and loss tangent 0.02. In the design, the resonant lengths of the arc-shaped monopole ' Z_1 ' ($Z_1 = Y_1 + L_3 + W_6 + g + g_1 + g_2 + g_3$), rectangular shaped monopole ' Z_2 ' ($Z_2 = L_4$) and the L-shaped monopole ' Z_3 ' ($Z_3 = L_2 + W_5$) are set close to half-wavelength, quarter-wavelength and quarter-wavelength respectively of the resonant frequencies which they are supposed to excite. These lengths are calculated by using Equations (1)–(4) and then optimized. Table 3 shows the resonances predicted by equations and those by simulations.

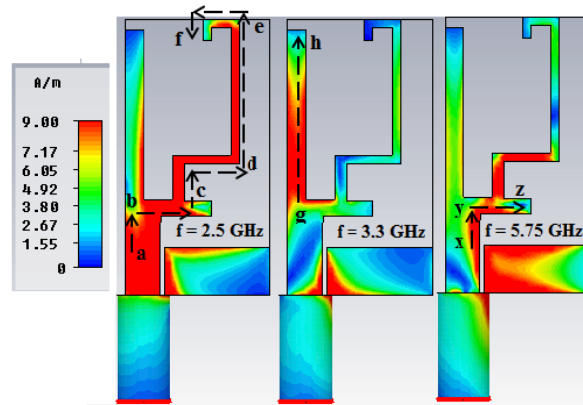


Figure 8. Simulated surface current distribution of the proposed antenna at 2.5 GHz, 3.3 GHz and 5.75 GHz.

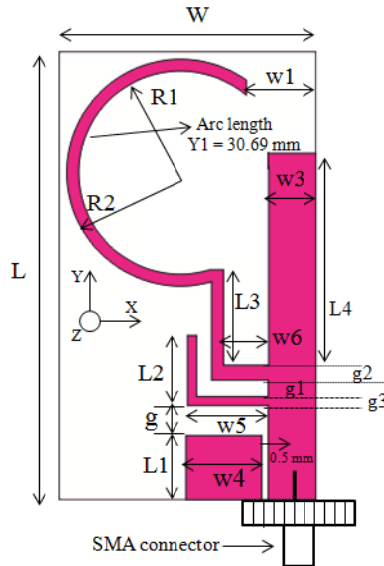


Figure 9. Geometry of the new ACS-Fed tri-band antenna.

Table 3. Comparison of predicted and simulated resonance for the proposed arcstrip antenna.

	f_1 (GHz)	f_2 (GHz)	f_3 (GHz)
Simulated	1.86	3.35	5.3
Calculated	1.98	3.25	5.2

They show good agreement. All the three resonant frequencies can be tuned independently by varying the lengths of the individual radiating strips. The optimized parameter values of the antenna are given in Table 4. The simulated -10 dB impedance bandwidths (Figure 10) are about 120 MHz from 1.8–1.92 GHz, 550 MHz from 3.2–3.75 GHz and 1.8 GHz from 5.0–6.8 GHz which can be used for 1800 MHz Digital Cordless Phones, PCS 1900 MHz, 3.5/5.5 GHz WiMAX, 5.2/5.8 GHz WLAN applications.

The simulated surface current distributions on the radiating monopoles at the three resonant frequencies, i.e., 1.85 GHz, 3.4 GHz, and 5.4 GHz, are shown in Figure 11. For the 1.85 GHz resonance, a large surface current distribution is observed on the arc shaped monopole branch (Z_1). This indicates that the arc-shaped monopole branch is the key radiating element to excite the 1.85 GHz resonant mode at $\lambda_g/2$. For the 3.4 GHz resonance, from the figure it is observed that more surface current is

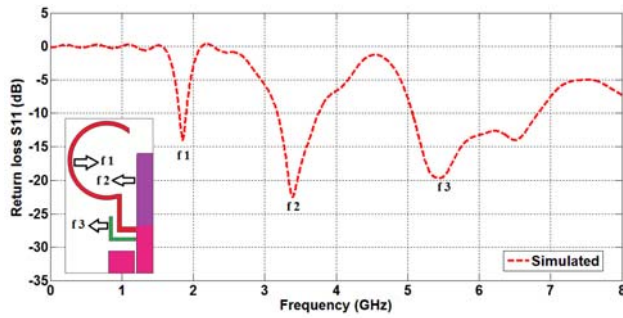


Figure 10. Simulated return loss against frequency.

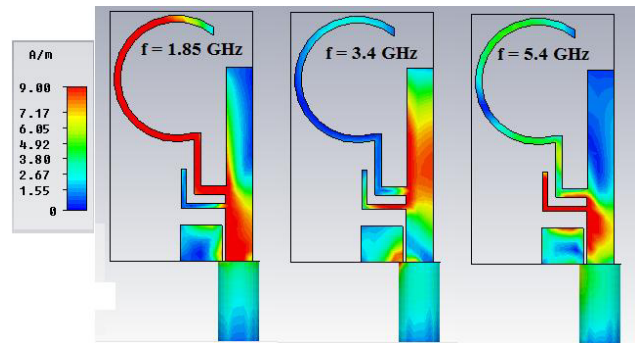
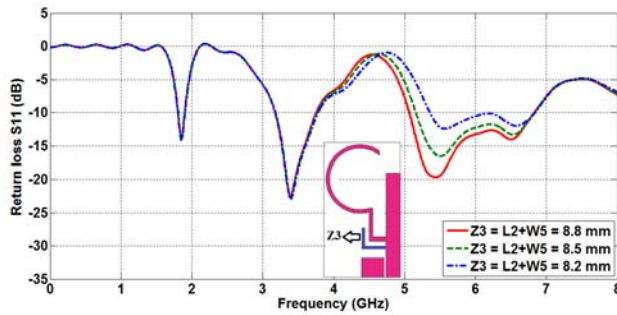
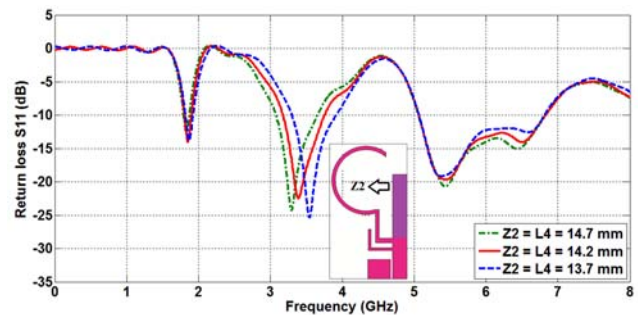


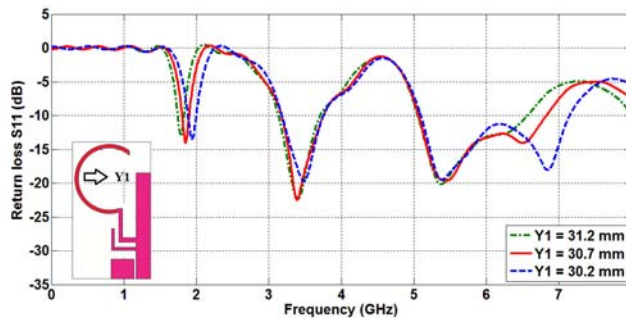
Figure 11. Simulated surface current distributions of the antenna at 1.85 GHz, 3.4 GHz, and 5.4 GHz.



(a)



(b)



(c)

Figure 12. (a). Simulated reflection coefficients of the proposed antenna with varied Z_3 . (b) Simulated reflection coefficients of the proposed antenna with varied Z_2 . (c) Simulated reflection coefficients of the proposed antenna with varied Y_1 .

Table 4. Optimized parameter values (in mm).

Parameter	L	W	L_1	L_2	L_3	L_4	W_1	W_3	W_4
Value (mm)	30	17.2	4.3	4.1	6.4	14.2	4.7	3.2	5
Parameter	W_5	W_6	R_1	R_2	G	g_1	g_2	g_3	
Value (mm)	4.7	3	6.8	7.6	2	1.1	1	0.6	

concentrated on the vertical rectangular shaped monopole (Z_2), and very less current density is present on the other radiating branches, implying that the resonance is because of the $\lambda_g/4$ length strip. Finally, at 5.4 GHz, a high current density on the L-shaped branch is observed, which indicates that the third operating band of the proposed antenna is due to the $\lambda_g/4$ length L-shaped monopole.

To demonstrate that the resonances in this design are independently tunable, similar to the previous design, a parametric analysis is performed. Figure 12(a) shows the simulated return losses of the antenna when the length of the L-shaped branch ' Z_3 ' is varied. It is shown that the third resonant frequency shifts towards higher frequencies as Z_3 is decreased while the first and second bands are not affected. A significant effect on the return loss magnitude and bandwidth of the third operating band is also observed when Z_3 changes from 8.8 mm to 8.2 mm. This clearly indicates that the length of the L-shaped branch determines the third resonant frequency of the proposed antenna. The effects of variations in the lengths Z_2 and Y_1 on the return loss are studied next and given in Figures 12(b) & 12(c), respectively. From Figure 12(b), it can be concluded that with an increase in the rectangular branch length Z_2 , the second resonant frequency shifts to lower side whereas the first and third resonant modes are not affected. Similarly from Figure 12(c), it is noticed that the first resonant frequency shifts to the lower side as the arc length Y_1 is increased while the second and third bands are affected slightly.

6. CONCLUSION

A technique to design very compact ACS-fed antenna for multi-band operation is proposed, discussed, and the fabricated prototype is tested experimentally. The proposed design has three different simple radiating elements that can excite the desired resonant frequencies. The resonances are independently tunable. The measured impedance bandwidths are about 200 MHz from 2.40–2.60 GHz, and 2800 MHz from 3.2–6.0 GHz. The good return loss characteristics, compact size with simple geometry, wide impedance bandwidth with omnidirectional radiation patterns along with acceptable peak gains make the proposed antenna a suitable candidate for 2.4 GHz Bluetooth/WiBree/Zigbee, 2.4/5.2/5.8 GHz WLAN, 3.5/5.5 GHz WiMAX, 5.9 GHz WAVE and 4.9 GHz US public safety system applications. The technique is validated by designing another similar antenna operation in 1.8/1.9 PCS, 3.5/5.5 GHz WiMAX, 5.2/5.8 GHz WLAN bands. Thus, this technique can be utilized at any desired multi-band/wideband application.

ACKNOWLEDGMENT

The authors like to acknowledge vice-chancellor Symbiosis International University (DU), Pune for continuous support. Authors also acknowledge Rajas Khokle for his technical suggestions.

REFERENCES

1. Sun, X. L., L. Liu, S. W. Cheung, and T. I. Yuk, "Dual-band antenna with compact radiator for 2.4/5.2/5.8 GHz WLAN applications," *IEEE Transactions on Antennas and Propagation*, Vol. 60, No. 12, 5924–5931, 2012.
2. Teng, X. Y., X. M. Zhang, Z. X. Yang, Y. Wang, Y. Li, Q. F. Dai, and Z. Zhang, "A compact CPW-fed omni-directional monopole antenna for WLAN and RFID applications," *Progress In Electromagnetics Research Letters*, Vol. 32, 91–99, 2012.

3. Lin, C. C., E. Z. Yu, and C. Y. Huang, "Dual-band rhombus slot antenna fed by CPW for WLAN applications," *IEEE Antennas and Wireless Propagation Letters*, Vol. 11, 362–364, 2012.
4. Sun, X. L., S. W. Cheung, and T. I. Yuk, "A compact monopole antenna for WLAN applications," *Microwave and Optical Technology Letters*, Vol. 56, No. 2, 469–475, 2014.
5. Tsai, L. C., "A triple-band bow-tie-shaped CPW-fed slot antenna for WLAN applications," *Progress In Electromagnetics Research C*, Vol. 47, 167–171, 2014.
6. Liu, W. C., C. M. Wu, and N. C. Chu, "A compact CPW-fed slotted patch antenna for dual-band operation," *IEEE Antennas and Wireless Propagation Letters*, Vol. 9, 110–113, 2010.
7. Liu, W. C. and W. R. Chen, "CPW-fed compact meandered patch antenna for dual-band operation," *Electronics Letters*, Vol. 40, No. 18, 1094–1095, 2004.
8. Deepu, V., R. Sujith, S. Mridula, C. K. Aanandan, K. Vasudevan, and P. Mohanan, "ACS fed printed F-shaped uniplanar antenna for dual band WLAN applications," *Microwave and Optical Technology Letters*, Vol. 51, No. 8, 1852–1856, 2009.
9. Huang, C. Y. and E. Z. Yu, "A slot-monopole antenna for dual-band WLAN applications," *IEEE Antennas and Wireless Propagation Letters*, Vol. 10, 500–502, 2011.
10. Zhao, G., F. S. Zhang, Y. Song, Z. B. Weng, and Y. C. Jiao, "Compact ring monopole antenna with double meander lines for 2.4/5 GHz dual-band operation," *Progress In Electromagnetics Research*, Vol. 72, 187–194, 2007.
11. Song, Y., Y. C. Jiao, X. M. Wang, Z. B. Weng, and F. S. Zhang, "Compact coplanar slot antenna fed by asymmetric coplanar strip for 2.4/5 GHz WLAN operations," *Microwave and Optical Technology Letters*, Vol. 50, No. 12, 3080–3083, 2008.
12. Xu, Y., Y. C. Jiao, and Y. C. Luan, "Compact CPW-fed printed monopole antenna with triple-band characteristics for WLAN/WiMAX applications," *Electronics Letters*, Vol. 48, No. 24, 1519–1520, 2012.
13. Naidu, P. V. and R. Kumar, "A small CPW-fed dual-band rupee shaped antenna for WiMAX and WLAN applications," *International Journal of Microwave and optical Technology*, Vol. 10, No. 1, 6–12, 2015.
14. Naidu, P. V. and R. Kumar, "A compact dual-band octagonal slotted printed monopole antenna for WLAN/WiMAX and UWB applications," *Journal of Microwaves, Optoelectronics and Electromagnetic Applications*, Vol. 14, No. 1, 1–13, 2015.
15. Yuan, B., P. Gao, S. He, L. Xu, and H. T. Guo, "A novel triple-band rectangular ring antenna with two L-shaped strips for WiMAX and WLAN applications," *Progress In Electromagnetics Research C*, Vol. 40, 15–24, 2013.
16. Zhang, X. Q., Y. C. Jiao, and W. H. Wang, "Miniature triple-band CPW-fed monopole antenna for WLAN/WiMAX applications," *Progress In Electromagnetics Research Letters*, Vol. 31, 97–105, 2012.
17. Xiong, L., P. Gao, and S. X. Han, "Compact triple-frequency planar monopole antenna for WiMAX/WLAN applications," *Progress In Electromagnetics Research Letters*, Vol. 34, 43–51, 2012.
18. Xie, J. J., X. S. Ren, Y. Z. Yin, and S. L. Zuo, "Rhombic slot antenna design with a pair of straight strips and two \cap -shaped slots for WLAN/WiMAX applications," *Microwave and Optical Technology Letters*, Vol. 54, No. 6, 1466–1469, 2012.
19. Liu, Z. Y., Y. Z. Yin, S. F. Zheng, W. Hu, L. H. Wen, and Q. Zou, "A compact CPW-fed monopole antenna with a U-shaped strip and a pair of L-slits ground for WLAN and WiMAX applications," *Progress In Electromagnetics Research Letters*, Vol. 16, 11–19, 2010.
20. Zhao, Q., S. X. Gong, W. Jiang, B. Yang, and J. Xie, "Compact wide-slot tri-band antenna for WLAN/WiMAX applications," *Progress In Electromagnetics Research Letters*, Vol. 18, 9–18, 2010.
21. Ren, X., S. Gao, and Y. Yin, "Compact tri-band monopole antenna with hybrid strips for WLAN/WiMAX applications," *Microwave and Optical Technology Letters*, Vol. 57, No. 1, 94–99, 2015.
22. Ren, F. C., F. S. Zhang, J. H. Bao, B. Chen, and Y. C. Jiao, "Compact triple-frequency slot antenna for WLAN/WiMAX operations," *Progress In Electromagnetics Research Letters*, Vol. 26,

- 21–30, 2011.
23. Song, Y., Y. C. Jiao, G. Zhao, and F. S. Zhang, “Multiband CPW-fed triangle-shaped monopole antenna for wireless applications,” *Progress In Electromagnetics Research*, Vol. 70, 329–336, 2007.
 24. Naidu, P. V. and R. Kumar, “Design of a compact ACS-fed dual band antenna for Bluetooth/WLAN and WiMAX applications,” *Progress In Electromagnetics Research C*, Vol. 55, 63–72, 2014.
 25. Chen, H., Y. Z. Yin, and J. Wu, “Compact tri-band meandered ring monopole antenna with two embedded strips for WLAN/WiMAX applications,” *Progress In Electromagnetics Research Letters*, Vol. 45, 63–67, 2014.
 26. Li, B., Z. H. Yan, and T. L. Zhang, “Triple-band slot antenna with U-shaped open stub fed by asymmetric coplanar strip for WLAN/WiMAX applications,” *Progress In Electromagnetics Research Letters*, Vol. 37, 123–131, 2013.
 27. Li, Y., W. Li, and R. Mittra, “A compact ACS-fed dual-band meandered monopole antenna for WLAN and WiMAX applications,” *Microwave and Optical Technology Letters*, Vol. 55, No. 10, 2370–2373, 2013.
 28. Li, Y., W. Li, and R. Mittra, “Miniaturization of ACS-fed dual-band antenna with loaded capacitance terminations for WLAN applications,” *IEICE Electronics Express*, Vol. 10, No. 15, 20130455–20130455, 2013.
 29. Li, Y., W. Li, and Q. Ye, “A compact asymmetric coplanar strip-fed dual-band antenna for 2.4/5.8 GHz WLAN applications,” *Microwave and Optical Technology Letters*, Vol. 55, No. 9, 2066–2070, 2013.
 30. Liu, Y. F., P. Wang, and H. Qin, “A compact triband ACS-fed monopole antenna employing inverted-L branches for WLAN/WiMAX applications,” *Progress In Electromagnetics Research C*, Vol. 47, 131–138, 2014.
 31. Deepu, V., R. K. Raj, M. Joseph, M. N. Suma, and P. Mohanan, “Compact asymmetric coplanar strip fed monopole antenna for multiband applications,” *IEEE Transactions on Antennas and Propagation*, Vol. 55, No. 8, 2351–2357, 2007.
 32. Ashkarali, P., S. Sreenath, R. Sujith, R. Dinesh, D. D. Krishna, and C. K. Aanandan, “A compact asymmetric coplanar strip fed dual-band antenna for DCS/WLAN applications,” *Microwave and Optical Technology Letters*, Vol. 54, No. 4, 1087–1089, 2012.
 33. Zhang, Z., *Antenna Design for Mobile Devices*, John Wiley & Sons, 2011.